Contribution from the Afd. Anorganische Chemie, Universiteit Nijmegen, Toernooiveld, NL-6525 ED Nijmegen, The Netherlands,
Fachbereich Chemie, Philipps-Universität Marburg, Hans-Meerweinstrasse, D-3550 Marburg/Lahn, FRG,
and Institut für Anorganische Chemie, Universität Hannover, Callinstrasse 9, D-3000 Hannover 1, FRG

Cooperative Effects in π-Ligand-Bridged Dinuclear Complexes.
11. Three Different Positional Isomers of Paramagnetic (μ-[$\eta^{7:7}$-Bi(cyclooctatrienyl)])bis[(η^5-cyclopentadienyl)vanadium]: Strong Influence on Magnetic Properties Caused by the Different Kinds of Linkages[1]

Bernd Bachmann,[2a] Jürgen Heck,*[,2b] Gerd Meyer,[2c] Jürgen Pebler,[2a] and Thomas Schleid[2c]

Received June 28, 1991

Attempts to prepare the mononuclear sandwich complex CpVCot or its anion [CpVCot]$^-$ (Cp = cyclopentadienyl; Cot = cyclooctatetraene) reveal one red (**2**) and two green (**3**, **5**) paramagnetic dinuclear complexes of the general composition [CpV(C_8H_8)]$_2$. X-ray structures of the red isomer **2** (space group $P2_1/c$, with a = 8.2797 (6) Å, b = 7.9257 (5) Å, c = 14.3273 (9) Å, β = 93.416 (7)°, V = 989.33 Å^3, Z = 2, and R = 0.035) and the green isomer **5** (space group $C2/c$, with a = 21.7603 (12) Å, b = 7.7366 (6) Å, c = 12.3510 (9) Å, β = 92.434 (6)°, V = 2077.42 Å^3, Z = 4, and R = 0.038) establish different linkages between the C_8 rings of two mononuclear CpV(C_8H_8) sandwich units: via two metal attached carbon atoms for the red isomer **2** and via an sp^3–sp^3 carbon–carbon single bond endo-positioned with respect to the metal centers for the green isomer **5**. The linkage in the third but thermally unstable isomer **3**, which isomerizes to the red one, is explained by an sp^3–sp^3 carbon–carbon single bond in the exo position relative to the metal centers. Magnetic susceptibility measurements and ESR spectra manifest the importance of the linkage between the two mononuclear subunits: (i) the exchange interaction in the red compound **2** (J = −62 cm^{-1}) is enhanced by 1 order of magnitude relative to the green endo isomer **5** (J = −5 cm^{-1}); (ii) fluid-solution ESR spectra show highly resolved ^{51}V-hyperfine structures for the green isomers **3** and **5** whereas a corresponding solution ESR spectrum for **2** fails; (iii) from the solid-solution ESR spectrum of **2** a zero-field-splitting parameter D can be estimated, which is much larger than that calculated from the distance of the paramagnetic centers taking into account the point dipole approximation.

Introduction

Heterodinuclear μ-cyclooctatetraene (Cot) complexes [(L_nM)(L'_mM')](μ-Cot) have been described in great variety with electron-rich metals of groups 8–10 of the periodic table.[3] These compounds contain at least 34 valence electrons (ve) and are diamagnetic. Work in our laboratory, however, has established that complexes of the general composition [(CpCr)(L_nM)](μ-Cot) with less than 34 ve (L_n = Cp, (CO)$_3$, M = Co, Fe, Cr, W) normally are paramagnetic with one to three unpaired electrons, and show predominant localization of the unpaired electron(s) on the less noble metal.[4-6]

For the syntheses of most of these dinuclear μ-Cot compounds the mononuclear Cot complex CpCr(η^6-Cot)[7,8] has been shown to be very suitable. In order to make the metal combinations more varied, we attempted to use CpVCot (**1**) as a precursor complex. In **1** the Cot ligand may be linked with the metal center in an η^8-bonding mode, as in CpTiCot,[9] or in an η^6-fashion, which has been proven for CpCr(η^6-Cot).[8] Although the direct neighbors CpTiCot and CpCrCot have been well-known for quite a long time, the synthesis of CpVCot has not yet been published except for some unsuccessful attempts.[10]

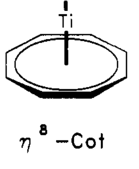

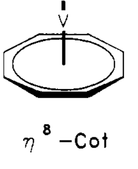

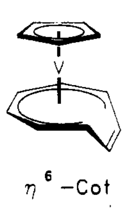

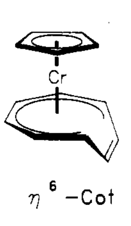

Experimental Section

All manipulations were carried out in a N_2 atmosphere and in N_2-saturated solvents. More details about the preparation of the solvents and about used apparative equipment are described elsewhere.[4] [V_2(THF)$_6$(μ-Cl)$_3$]$_2$[Zn_2Cl_6],[11] [V_2(THF)$_6$(μ-Cl)$_3$][$AlEt_2Cl_2$],[12] CpVCl$_2$PMe$_2$,[10] [CpVPEt$_3$Cl]$_2$,[13] CpV(η^6-$C_{10}H_8$),[14] and CpV(η^7-C_8H_9)[15] were produced by literature methods. Cot was purchased from BASF.

Preparation of [CpV(η^7-C_8H_8)]$_2$ (Red, 2). From VCl$_3$. A 3.74-g (10-mmol) sample of VCl$_3$(THF)$_3$ is dissolved in 100 mL of THF. At −50 °C, 50 mL of a THF solution containing 1.37 g (7.5 mmol) of K_2Cot is added dropwise. Subsequently, 881 mg (10 mmol) of solid NaCp is added to the reaction mixture, which is stirred for 18 h in the course of which the reaction mixture is allowed to warm up to room temperature. After 2 h of reflux the solvent is evaporated in vacuum and the solid residue is warmed up to 70 °C in high vacuum yielding 450 mg (26.5%) of vanadocene as sublimate. The residue is dissolved in toluene and filtered over a column packed with silylated SiO$_2$. The dark burgundy-colored filtrate is reduced in volume and overlayed with hexane. After storage over 2–3 days at −28 °C, 730 mg (33%) of dark red crystals of **2** are obtained.

From CpVCl$_2$(PMe$_3$). A 2.38-g (7.02-mmol) sample of CpVCl$_2$(PMe$_3$)$_2$ is dissolved in 150 mL of THF. After the solution was cooled to −78 °C, 18.5 mL of a THF solution containing 7.02 mmol of K_2Cot is added dropwise during 3 h. The reaction mixture is allowed to warm up to room temperature within 24 h and evaporated to dryness. The solid residue is continuously extracted with hot hexane until the extract becomes colorless. The hexane extract is cooled to −78 °C, and the resulting dark red crystalline material is recrystallized from a toluene/hexane mixture: yield 830 mg (54%) of **2**; mp 210 °C. Anal. Calcd for $C_{26}H_{26}V_2$: C, 70.91; H, 5.95. Found: C, 71.71; H, 6.19. EI-MS, m/e (%): 441 (19.3), 440 (59.9), 323 (23.3), 257 (9.9), 231 (22.6), 221 (6.6), 220 (42.6), 218 (18.0), 207 (70.3), 181 (35.4), 129 (33.7), 116 (100), 91 (5.5), 51 (26.8). High resolution MS: calcd, 440.0893; found, 440.0914.

---

(1) Part 10. Abriel, W.; Baum, G.; Burdorf, H.; Heck, J. *Z. Naturforsch. B.* **1991**, *46*, 841.

(2) (a) Philipps-Universität Marburg. (b) Universiteit Nijmegen. (c) Universität Hannover.

(3) Geiger, W. E.; Salzer, A.; Edwin, J.; von Philipsborn, W.; Piantini, U.; Rheingold, A. L. *J. Am. Chem. Soc.* **1990**, *112*, 7113 and literature cited therein.

(4) Bachmann, B.; Hahn, F.; Heck, J.; Wünsch, M. *Organometallics* **1989**, *8*, 2523.

(5) Heck, J.; Hermans, P. M. J. A.; Scholten, A. B.; Meyer, G.; Staffel, Th. *Z. Anorg. Allgem. Chem.*, in press.

(6) Heck, J.; Hermans, M. In *Chemiedozententagung*; Döpp, D., Ed.; Universität-GH-Duisburg: Duisburg, Germany, 1991; Abstract A12.

(7) Müller, J.; Mehnig, H. *J. Organomet. Chem.* **1975**, *96*, 83.

(8) Heck, J.; Rist, G. *J. Organomet. Chem.* **1988**, *342*, 45.

(9) Van Oven, H. O.; De Liefde Meijer, H. J. *J. Organomet. Chem.* **1969**, *19*, 373.

(10) Niemann, J.; Teuben, J. H.; Huffman, J. C.; Caulton, K. G. *J. Organomet. Chem.* **1983**, *255*, 193.

(11) Köhler, F. H.; Prössdorf, W. *Z. Naturforsch., B* **1977**, *32*, 1026. Bouma, R. J.; Teuben, J. H.; Beukema, W. R.; Bansemer, R. L.; Huffmann, J. C.; Caulton, K. G. *Inorg. Chem.* **1983**, *23*, 2715.

(12) Cotton, F. A.; Duraj, S. A.; Manzer, L. E.; Roth, W. J. *J. Am. Chem. Soc.* **1985**, *107*, 3850.

(13) Niemann, J.; Teuben, J. H. *Organometallics* **1986**, *5*, 1149. Niemann, J.; Teuben, J. H.; Hulsbergen, F. B.; DeGraaff, R. A. G.; Reedijk, J. *Inorg. Chem.* **1987**, *26*, 2376.

(14) Rüssler, W. Dissertation, Ruhr-Universität Bochum, Bochum, FRG, 1986.

(15) Bachmann, B.; Heck, J. *Organometallics* **1991**, *10*, 1373.

0020-1669/92/1331-0607$03.00/0

Table I. Crystallographic Data for **2** and **5**

	2	**5**
chem formula	$C_{26}H_{26}V_2$	$C_{26}H_{26}V_2$
fw	440.1	440.1
cryst color	red	green
space group	$P2_1/c$ (No. 14)	$C2/c$ (No. 15)
cryst syst	monoclinic	monoclinic
cell dimens		
a, Å	8.7279 (6)	21.7603 (12)
b, Å	7.9257 (5)	7.7366 (6)
c, Å	14.3273 (9)	12.3510 (9)
β, deg	93.416 (7)	92.434 (6)
Z, molecules/cell	2	4
V, Å^3	989.33	2077.43
D_{calcd}, g/cm^3	1.478	1.408
T, K	293	293
μ, cm^{-1}	8.90	8.48
2Θ range, deg	6–60	4–56
F(000)	456	912
no. of indep reflcns meas	3473	2395
no. of obs reflcns with $\|F_o\| \geq n\,\sigma(F_o)$	3113 (n = 2)	2339 (n = 1.5)
R^a	0.035	0.038
$R_w{}^b$	0.029	0.029

[a] $R = \sum||F_o| - |F_c||/|F_o|$. [b] $R_w = \sum||F_o| - |F_c||\, w^{1/2}/|F_o|\, w^{1/2}$, $w = k[\sigma(F_o)^{-2}]$; k = 0.947 (**2**), 0.018 (**5**).

Preparation of [CpV(η^7-C_8H_8)]$_2$ (Green, 3). The preparation of **3** occurs in strict analogy to the reaction described in ref 14: 1.13 g (4.63 mmol) of CpV(η^6-$C_{10}H_8$) is dissolved in 50 mL of hexane. This solution is stored in a Schlenk filter with a slight N_2 stream flowing through the bottom of the filter. At room temperature 0.55 mL (4.7 mmol) of Cot is added. After 2 h the precipitated green material is filtered off and washed with small amounts of hexane. A total yield of 550 mg (54%) of **3** is obtained.

Preparation of [CpV(η^7-C_8H_8)]$_2$ (Green, 5). A 0.9-g (1.67-mmol) sample of [CpVCl(PEt$_3$)]$_2$ is dissolved in 50 mL of THF. At −78 °C 7.1 mL of a THF solution containing 1.67 mmol of K_2Cot is added. After being warmed up to room temperature and stirred for 48 h, the reaction mixture is evaporated to dryness. The residue is first extracted with hexane, from which only few milligrams of (CpV)$_2$(μ-Cot) can be obtained. Subsequently, the residue is extracted with toluene until the toluene extract is colorless. The extract is restricted, overlayed with hexane, and stored at −28 °C for 2 days: yield 210 mg (57.1%) of green needles of **5**; mp > 240 °C dec. Anal. Calcd for $C_{26}H_{26}V_2$: C, 70.91; H, 5.95. Found: C, 70.97; H, 6.04. EI-MS, *m/e* (%): 441 (5.2), 440 (19.2), 323 (1.1), 257 (1.6), 231 (31.0), 221 (12.9), 220 (100), 218 (5.7), 207 (21.6), 181 (5.4), 129 (5.4), 116 (87.8), 91 (1.6), 90 (4.5), 51 (12.3).

The electronic absorption spectra were obtained from 10^{-4}–10^{-3} M hexane and THF solutions of **2**, **4**, and **5** (Perkin-Elmer Lambda 2 UV/vis spectrometer). Since these compounds are very air sensitive, the purity of the samples was proven by permitting a short air contact after the first measurement. Subsequent recording of the spectra reveals absorption maxima other than those in the original sample.

The magnetic susceptibility of the dinuclear compounds **2** and **5** was determined from powdered samples in the range 4.2–300 K for **2** and in the range 4–140 K for **5** in external fields up to 2 T on a vibrating sample magnetometer, Model 155 (PAR), using a variable-temperature cryostat from Janis Research Co.

X-ray diffraction studies were performed with single crystals of **2** and **5** obtained from slow crystallization from hexane at a small temperature gradient. The proper crystals were sealed under N_2 in a thin walled quartz capillary. The X-ray data were collected on a four-circle Siemens-Stoe AED 2 instrument with graphite-monochromated Mo Kα radiation (λ = 0.7107 Å) by using the $\omega/2\theta$ scan technique with a variable learnt-profile method.[16] Lorentz and polarization factors were applied, and corrections for the absorption were made. The lattice constants were obtained from Guinier–Simon data.[17,18] The crystal structures were solved by Patterson for V atoms and difference Fourier syntheses for C and H atoms.[19] The V and C positions are refined by anisotropic thermal parameters whereas the H positions are refined by isotropic thermal parameters (see supplementary material). Scattering factors are taken from ref 20. Crystallographic data are given in Table I.

Results

Preparations. The first attempt to prepare **1** was carried out by a one-pot reaction, owing to the success of the synthesis of the mononuclear complex (C_5Me_5)Cr(η^6-Cot)[8] starting from a vanadium(III) halide (eq 1). The isolated product **2** is dark red in color and paramagnetic and shows the intended empirical formula of **1**, but is dinuclear. The same compound is obtained from reaction 2 starting with the proper V(III) half-sandwich complex CpVCl$_2$(PEt$_3$)$_2$.[10]

$$VCl_3(THF)_3 + NaCp + K_2Cot \xrightarrow[\substack{-NaCl\\2KCl}]{} \underset{\mathbf{2}}{(CpVC_8H_8)_2} \text{ (red)} \tag{1}$$

$$CpVCl_2(PEt_3)_2 + K_2Cot \rightarrow \mathbf{2} + 2KCl + 2PEt_3 \tag{2}$$

From these reactions no clue to the formation of **1** was revealed. However, Jonas and co-workers have described the synthesis of **1** by a ligand-exchange reaction between CpV(η^6-$C_{10}H_8$) ($C_{10}H_8$ = naphthalene) and Cot (eq 3).[14,22a,b] A revision of this reaction confirms the formation of the described paramagnetic green complex with the desired empirical formula of **1**, but as shown by means of ESR spectroscopy (vide infra) this complex again is dinuclear.

$$CpV(C_{10}H_8) + Cot \xrightarrow[-C_{10}H_8]{} {}^1\!/_2\underset{\mathbf{3}}{(CpVC_8H_8)_2} \text{ (green)} \tag{3}$$

As can be followed by ESR, **3** thermally isomerizes in solution to the red compound **2** (eq 4): at elevated temperatures the ESR spectrum of the fluid solution of **3** disappears and the solid-solution spectrum of **2** can be recognized (vide infra).

$$\mathbf{3} \xrightarrow[60\ °C/3\ h]{toluene} \mathbf{2} \tag{4}$$

Apparently, the mononuclear sandwich compound CpVCot is not sufficiently stable to be isolated. Therefore, it was decided to attempt to synthesize the anion [CpVCot]$^-$, which should be isoelectronic with CpCr(η^6-Cot).[22b] The formation of [CpVCot]$^-$ was expected from the reaction of K_2Cot with [CpVCl(PEt$_3$)]$_2$[15] (eq 5). However, reaction 5 yields another paramagnetic dinuclear complex **5** of green color with the same formula as **2** and **3**, which in contrast to **3** is thermally stable.

$$[CpVCl(PEt_3)]_2 + K_2Cot \rightarrow {}^1\!/_2\underset{\mathbf{5}}{(CpVC_8H_8)_2} \text{ (green)} \tag{5}$$

X-ray Structure. The molecular and crystal structures of **2** (red) and **5** (green) have been established from single-crystal X-ray diffraction studies. The molecular structures are shown in Figure 1, the fractional positional parameters are listed in Table II, and selected bond lengths and angles are given in Table III.

Remarkably, both compounds are composed of two almost identical (η^5-cyclopentadienyl)(η^7-cyclooctatrienyl)vanadium units. The Cp ligands in both complexes indicate a ring-to-metal bonding of the normal η^5-fashion with C–C and V–C bond lengths of 1.39

---

(16) Clegg, W. *Acta Crystallogr., Sect. A* **1981**, *37*, 22.

(17) Simon, A. *J. Appl. Crystallogr.* **1970**, *3*, 11.

(18) Soose, J.; Meyer, G. SOS—programs for the refinement of lattice constants from Guinier data. Giessen, FRG, 1980.

(19) Sheldrick, G. M. SHELX-76 and SHELX-86—programs for the determination of crystal structures from X-ray diffractometer data. Cambridge, U.K., 1976, Göttingen, FRG, 1986.

(20) Cromer, D. T.; Mann, J. B. *Acta Crystallogr., Sect. A* **1968**, *24*, 321. Cromer, D. T.; Liberman, D. *J. Chem. Phys.* **1970**, *53*, 1891.

(21) Fischer, R. X.; Tillmanns, E. *Acta Crystallogr., Sect. C* **1988**, *44*, 775.

(22) (a) Jonas and co-workers obtained a paramagnetic green complex, which has been interpreted as the desired mononuclear complex CpVCot (**1**) with χ_M(296 K) = 1.8 × 10^{-3} cm^3/mol (μ = 2.07 μ_B). The thermal instability of **3** and formation of **2** has been attributed to a dimerization of **1** (see ref 14). **2** was also synthesized by another route taking CpV(η^3-allyl)$_2$ as a precursor (Jonas, K.; Duff, W. Unpublished results). The structural data of **2** determined by Jonas and co-workers (see ref 14) are in very good agreement with the structural data published in this work. However, the interpretation of the Cot–V bonding mode is different from ours. (b) Another synthetic route to prepare [CpVCot]$^-$ is reported by: Wiskamp, V. Dissertation, Ruhr-Universität Bochum, Bochum, FRG, 1981.

Table II. Final Fractional Atomic Coordinates and Coefficients of Equivalent Thermal Displacement Factors U_{eq}[a] of **2** and **5**[b]

	x/a	y/b	z/c	U_{eq}
		Complex **2**		
V	0.26176 (3)	0.14826 (3)	0.37863 (2)	297 (1)
C1	0.4718 (2)	0.0863 (2)	0.4923 (1)	324 (4)
C2	0.3339 (2)	0.1410 (2)	0.5293 (1)	376 (4)
C3	0.2474 (2)	0.2897 (2)	0.5091 (1)	441 (5)
C4	0.2376 (2)	0.4054 (2)	0.4314 (1)	491 (5)
C5	0.3024 (2)	0.4118 (2)	0.3428 (1)	486 (5)
C6	0.4135 (2)	0.5128 (2)	0.3018 (1)	449 (5)
C7	0.5149 (2)	0.2019 (2)	0.3469 (1)	401 (5)
C8	0.5694 (2)	0.2172 (2)	0.4479 (1)	396 (5)
C11	0.0847 (2)	0.0962 (2)	0.2589 (1)	455 (5)
C22	0.0163 (2)	0.0697 (2)	0.3434 (1)	471 (5)
C33	0.9056 (2)	0.0652 (2)	0.6104 (1)	491 (6)
C44	0.7888 (2)	0.3801 (2)	0.1668 (1)	478 (6)
C55	0.2045 (2)	0.5193 (2)	0.7522 (1)	446 (5)
		Complex **5**		
V	0.12695 (1)	0.23032 (4)	0.11505 (2)	376 (1)
C1	0.46160 (8)	0.2754 (3)	0.9967 (1)	438 (6)
C2	0.41377 (8)	0.1881 (3)	0.0422 (1)	506 (6)
C3	0.35377 (8)	0.2489 (3)	0.0569 (1)	541 (7)
C4	0.31954 (8)	0.3865 (3)	0.0116 (1)	554 (7)
C5	0.32702 (8)	0.5099 (3)	0.9281 (1)	549 (7)
C6	0.37753 (8)	0.5513 (2)	0.8621 (1)	531 (7)
C7	0.43855 (7)	0.5059 (2)	0.8826 (1)	427 (5)
C8	0.46702 (7)	0.4680 (2)	0.9919 (1)	392 (6)
C11	0.3439 (1)	0.2294 (3)	0.7100 (2)	745 (10)
C22	0.4010 (1)	0.1522 (3)	0.7276 (2)	725 (8)
C33	0.3942 (1)	0.0175 (3)	0.8013 (2)	759 (11)
C44	0.3323 (1)	0.0141 (3)	0.8290 (2)	741 (9)
C55	0.3019 (1)	0.1438 (3)	0.7739 (2)	748 (9)

[a] Equivalent displacement factor of the type $U_{eq} = {}^1/_3[U_{22} + (1/\sin^2\beta)(U_{11} + U_{33} + 2U_{13}\cos\beta)]^{21}$ (U_{eq} in Å^2 × 10^4). [b] The final fractional coordinates and coefficients of the isotropic thermal displacement factors of the H atoms can be obtained from the supplementary material.

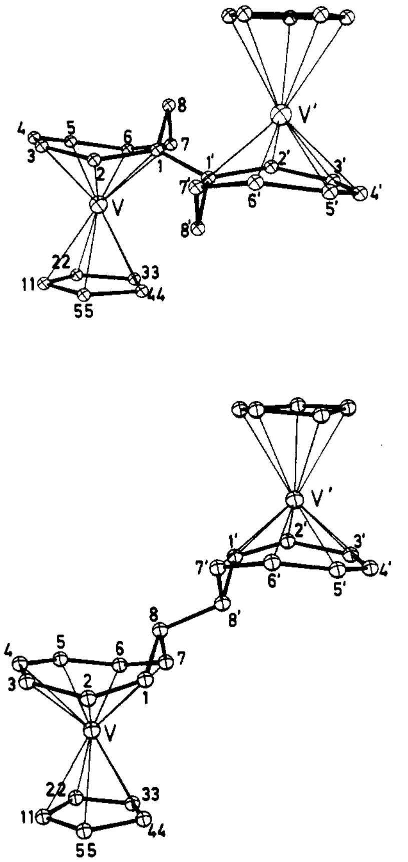

Figure 1. Molecular structures of **2** (above) and **5** (below) obtained from X-ray structure analysis containing the non-hydrogen atoms only.

Scheme I

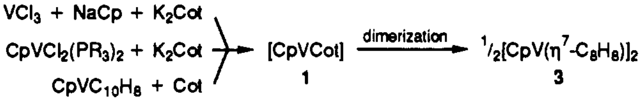

± 0.02 and 2.26 ± 0.02 Å, respectively. The C_8 ligands show an η^7-bonding mode with the sp^3 carbon atom C8 exo positioned with respect to the metal center. The C–C bond lengths to the adjacent carbon atoms C1 and C7 with 1.50 ± 0.01 Å attest to C–C single bonds, and the enclosed bond angles of 101° are considerably smaller than expected for a common tetrahedral angle at an sp^3 carbon atom.

The distances of the metal centers to the metal-attached carbon atoms C2–C6 are about 2.20 ± 0.01 Å whereas 2.32 Å is found for distances to the terminal carbon atoms C1 and C7, except for the distance V–C1 in **2**, which even is 2.43 Å. Nevertheless, this distance is still shorter than the longest V–C bond length in V(Cot)$_2$,[23] and the elongation is attributed to the bridging position

Table III. Selected Interatomic Distances (Å) and Angles (deg) in **2** and **5**

	2	**5**		**2**	**5**
		Distances			
V–V	5.7610 (4)	6.1758 (3)			
V–C1	2.429 (2)	2.322 (2)	C1–C2	1.412 (2)	1.380 (3)
V–C2	2.213 (1)	2.193 (1)	C2–C3	1.420 (2)	1.407 (3)
V–C3	2.190 (1)	2.188 (1)	C3–C4	1.441 (2)	1.402 (3)
V–C4	2.188 (2)	2.185 (2)	C4–C5	1.421 (2)	1.420 (3)
V–C5	2.185 (2)	2.188 (2)	C5–C6	1.403 (2)	1.432 (2)
V–C6	2.200 (2)	2.200 (2)	C6–C7	1.380 (2)	1.386 (2)
V–C7	2.321 (2)	2.319 (1)	C7–C8	1.501 (2)	1.490 (2)
V–C8	2.859 (2)	2.837 (1)	C8–C1	1.507 (2)	1.496 (3)
			C1–C1′	1.466 (2)	
			C8–C8′		1.523 (2)
		Angles			
C7–C8–C1	101.3 (1)	101.6 (1)	C3–C4–C5	134.8 (2)	136.5 (2)
C8–C1–C2	117.6 (1)	124.4 (2)	C4–C5–C6	132.5 (1)	132.7 (2)
C1–C2–C3	129.3 (1)	127.5 (2)	C5–C6–C7	126.9 (1)	126.3 (1)
C2–C3–C4	133.8 (1)	133.1 (2)	C6–C7–C8	123.9 (1)	125.0 (1)
C2–C1–C1′	121.1 (1)		C8–C1–C1′	120.8 (1)	
C7–C8–C8′		114.1 (1)	C1–C8–C8′		113.2 (1)
		Angles between Best Planes[a]			
1[b]–2[c]	105.3 (1)	110.7 (1)	3–4[e]	175.4 (2)	174.6 (2)
2–3[d]	161.4 (1)	161.7 (1)			

[a] The maximum deviation of the carbon atoms are equal or smaller than ±0.02 Å for **2** and smaller than ±0.001 Å for **5** (see supplementary material). [b] Plane 1: C7–C8–C1. [c] Plane 2: C1–C2–C6–C7. [d] Plane 3: C2–C3–C5–C6. [e] Plane 4: C3–C4–C5.

Table IV. EPR and Magnetic Data for the Dinuclear Complexes **2**, **3**, **5**, and **7** as Well as the Mononuclear d^5 Vanadium Sandwich Complexes **4** and **6** and Data Obtained from Magnetic Measurements

	g values[a]			^{51}V-hyperfine coupling,[b] mT					
	g_{iso}	$g_\perp$	$g_\parallel$	a_{iso}	$A_\perp$	$A_\parallel$	$A(g = 4)$	10^4D,[c] cm^{-1}	J,[d] cm^{-1}
2	... (1.99)[d]	...	...	...	...	5.3	5.4	580	−62
3	1.985	nd[i]	1.98	4.18	nd	5.5 5.0	5.3	90	
5	1.983 (1.98)[d]	nd	1.98	4.02	nd	5.2 4.5	5.1	75	−5
4[e]	1.981	1.973 1.976	2.004	7.90	10.67 9.57	0.49	...	...	
6[f]	1.987	1.978	2.005	7.41	10.41	1.49	...	...	
7[g]	1.988	nd	nd	3.10			4.3	154	−6[h]

[a] ±0.001. [b] ±0.05 mT. [c] Estimated according to ref 25a. [d] Obtained from the best fits according to eq 6 (see Figure 5a,b). [e] From ref 15. [f] **6**: $CpVC_7H_7$, data taken from ref 24a. [g] **7**: [μ-($\eta^{6:6}$-biphenyl)] bis[(η^6-benzene)vanadium].[38] [h] Calculated from the temperature dependence of the line intensity of the half-field signal $\Delta m_s = 2$ (T_{max} = 10 K, see ref 45). [i] nd = not determined.

of C1 in **2**, evoking a steric repulsion of the adjacent CH functions of the two $CpV(\eta^7\text{-}C_8H_8)$ subunits which are facing one another, such as positions 2 and 8′ as well as positions 8 and 2′. The fairly long distances of the exo-positioned carbon atoms C8 to the metal centers in **2** and **5** (2.86 ± 0.01 Å) do not indicate any V–C8 bonding interaction. The average V–C bond lengths in the V-(η^7-C_8H_8) units agree well with the V–C distances in the V-(η^7-C_7H_7) unit of $CpV(\eta^7\text{-}C_7H_7)$ (**6**).[24] The latter, however, contains an ideal C_7 plane, whereas the η^7-cyclooctatrienyl ligands in **2** and **5** can be broken down into four planes and resemble a shallow boat with the steep bow of the sp^3 carbon atoms C8 (see Table III).

The most important feature of these structures are the different kinds of linkages between the $CpV(\eta^7\text{-}C_8H_8)$ subunits. In the green isomer **5** the mononuclear subunits are linked via an sp^3–sp^3 carbon–carbon single bond between C8 and C8′ "endo"-positioned with respect to the V centers with a C8–C8′ bond length of 1.523 Å. The red isomer **2** contains a bridge between the carbon atoms C1 and C1′ which are directly attached to the metal centers as well. The C1–C1′ bridge length in **2** is somewhat shorter (1.466 Å). The different kinds of linkages result in considerably different nonbonding V–V′ distances: 5.761 Å in the red isomer **2** and 6.176 Å in the green isomer **5**.

ESR Spectroscopy. Fluid solution spectra are obtained from the green dinuclear products (**3**, **5**) and are shown in Figure 2 together with the fluid-solution ESR spectrum of the mononuclear complex **4**. Unfortunately, a fluid-solution spectrum of the red isomer **2** is unobtainable. Whereas the mononuclear compound **4** only shows an eight-line pattern caused by the hyperfine (hf) interaction of the unpaired electron with one V nucleus [$I(^{51}V) = {}^7/_2$, $a(^{51}V)$ = 7.9 mT] (Figure 2A), 15-line hf structures (hfs) are recorded for **3** and **5** (Figure 2B,C) indicating equivalent coupling of the unpaired electrons with both of the V centers. The hf coupling constants of the dinuclear species **3** and **5** are very similar [$a(^{51}V,3)$ = 4.18 mT; $a(^{51}V,5)$ = 4.02 mT], and half as large as $a(^{51}V)$ of the mononuclear species **4**, while the isotropic g values of these three compounds are almost identical (g_{iso} = 1.985–1.981) (see also Table IV).

The most important features of the solid-solution spectra of **2**, **3**, and **5** (Figure 3) are the signals in the $g = 4$ region, consisting of a 15-line pattern similar to the pattern seen in the isotropic spectra. These resonance signals are caused by the $\Delta m_s = 2$ transitions, confirming a triplet state for the dinuclear isomers in solid solution.

From the hfs of the solid solution spectra of **2**, **3**, and **5** only limited data can be obtained (see Table IV), because of the jamming of signals in the $g = 2$ region produced by the overlap of the fine structure and corresponding ^{51}V hfs. The hfs of the red isomer **2** is of still lower resolution, and moreover, the $\Delta m_s = 1$ spectrum of the triplet species is superimposed with a doublet hfs resembling that for the mononuclear complex $CpV(\eta^7\text{-}C_8H_9)$ (**4**) in solid solution (see also magnetic susceptibility measurements). Hence, the zero-field-splitting parameters D in Table IV are only approximately determined from the experimental spectra.[25a]

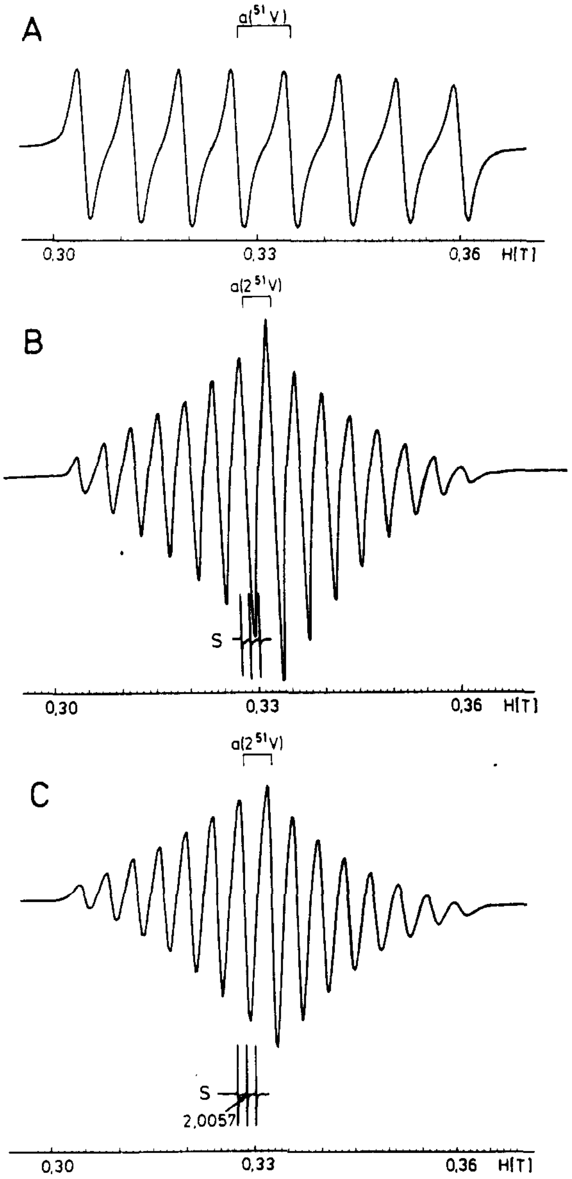

Figure 2. Fluid-solution ESR spectra of **4** (A), **3** (B), and **5** (C) (toluene, 293 K, X-band, S = reference, Fremy's salt $ON(SO_3K)_2$, g_{iso} = 2.0057).

---

(23) Gourier, D.; Samuel, E.; Bachmann, B.; Hahn, F.; Heck, J. *Inorg. Chem.*, in press.

(24) (a) Rettig, M. F.; Stout, C. D.; Klug, A.; Farnham, P. *J. Am. Chem. Soc.* **1970**, *92*, 5100. (b) Engbertson, G.; Rundle, R. E. *J. Am. Chem. Soc.* **1963**, *85*, 481.

Table V. UV/Vis Data for **2**, **4**, and **5**[a]

complex	abs max, nm (molar extinction coeff, cm^{-1} M^{-1})					
2	241 (23 200)[b]	273 sh	286 sh	321 sh	361 (12 300)	530 (4800)
	241 (24 300)[c]				360 (12 000)	529 (4970)
4	259 (14 000)[b]	296 sh	327 sh	380 sh	450 sh	670 (70)
5	256[b,d]	296 sh	329 sh			
	256 (27 900)[c]	296 sh	328 sh	388 sh	450 sh	670 (270)

[a] Absorption maxima denoted by sh (= shoulder) are determined by second derivatives of the absorption signals. [b] In hexane. [c] In THF. [d] Concentration not determined.

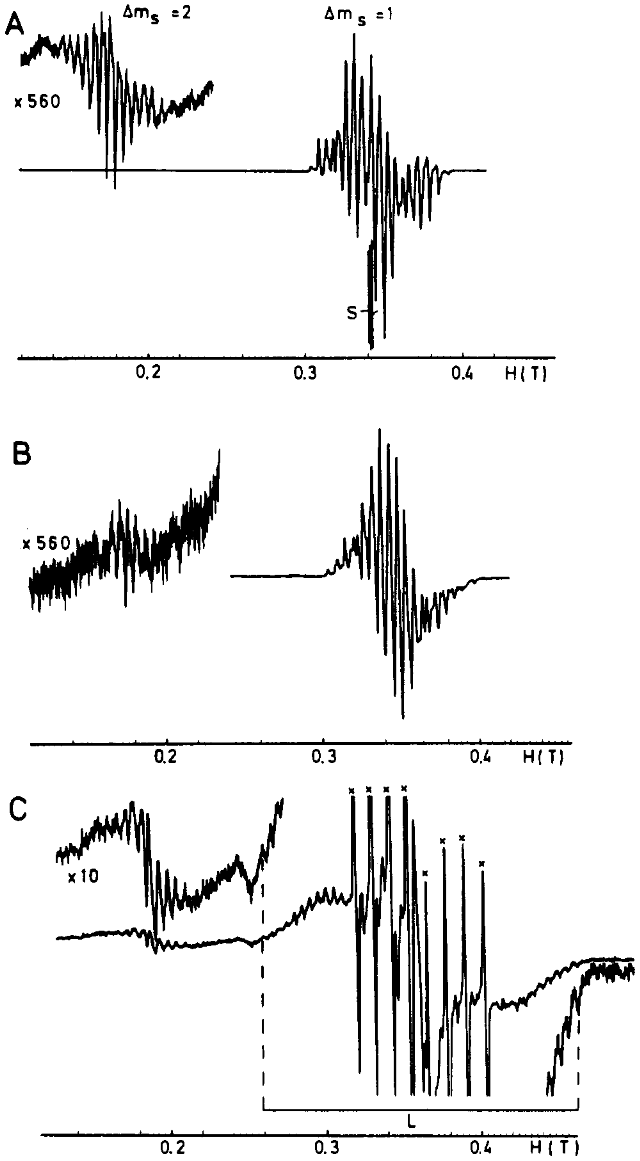

Figure 3. Solid-solution ESR spectra: (A) **5**; (B) **3**; (C) **2** (X-band, toluene, 130 K, × = doublet species (see text), S = reference, Fremy's salt).

Electronic Absorption Spectra. As can be seen from Figure 4 the electronic absorption spectra of the mononuclear species **4** and the green dinuclear one **5** are very similar (see also Table V) whereas the spectrum of the red dinuclear compound **2** is distinctly different especially above 300 nm: two new noticeable maxima appear at 361 and 530 nm for **2** from which the last absorption maximum may be responsible for the red color of **2**.

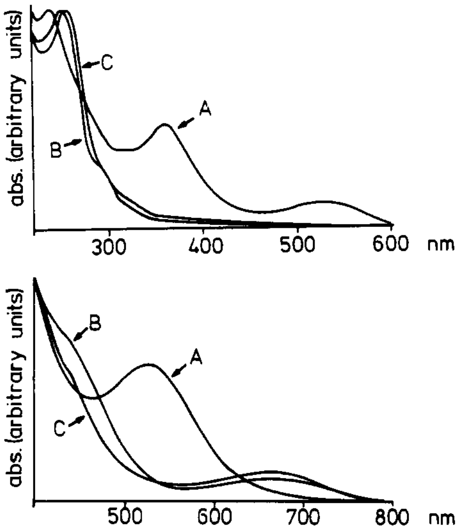

Figure 4. Electronic absorption spectra of **2** (A), **4** (B), and **5** (C) (hexane, 293 K).

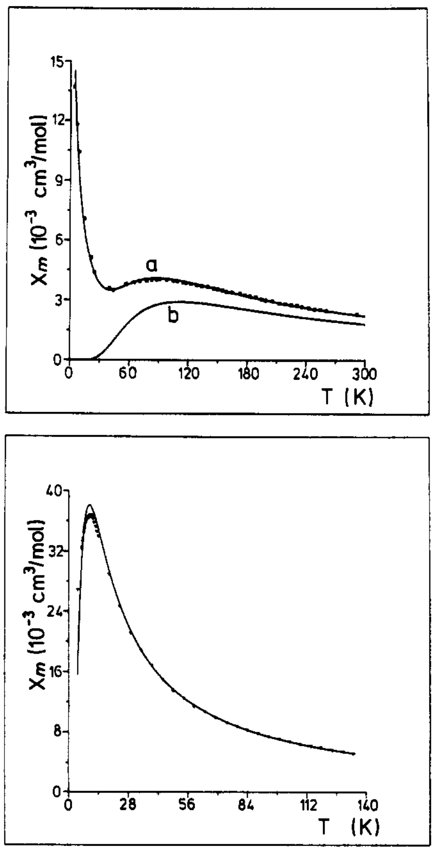

Figure 5. Temperature dependence of the magnetic susceptibility of a polycrystalline sample of **2** (above) [(a) fitted line according to eq 6 with regard to 16.7% doublet impurity; (b) line after deduction of the doublet impurity] and **5** (below).

Magnetic Susceptibility. The temperature-dependent magnetic susceptibility data for **2** and **5** are plotted in Figure 5. The

---

(25) (a) The energy separation of the fine components along the z direction (parallel to V–V vector) equals $2D$. Considering a ^{51}V-hf coupling constant $A_z(^{51}V)$ on the low- and high-field components, $2D$ is equal to $L - 14A_z(^{51}V)$, where L is the separation between the outermost lines on the low- and high-field sides of the $\Delta m_s = 1$ spectrum (see also Figure 7, included in the supplementary material). (b) Elschenbroich, Ch.; Heck, J. *Angew. Chem.* **1981**, *93*, 278.

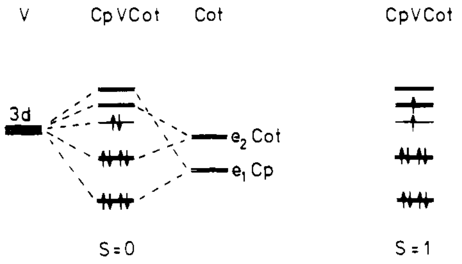

Figure 6. Qualitative MO description of the frontier orbitals in CpVCot with $S = 0$ (left) and $S = 1$ (right) derived from INDO-MO calculations of CpTiCot (see ref 28c).

observed broad maxima in the molecular susceptibility χ_m of **2** as well as of **5** are undoubtedly due to short-range (antiferromagnetic) interaction between metal atoms within the dinuclear compounds. The intramolecular spin-spin interaction of the dinuclear complexes can be treated quantitatively using the approach outlined by Van Vleck.[26] The Hamiltonian in use for metal-metal interaction in the dinuclear compounds is the isotropic operator $H = -2JS_1S_2$.[26d] We adopt the convention that negative exchange interaction J refers to a spin-singlet ground state and a spin triplet $2J$ in energy above the singlet. Thus, the isothermal magnetic susceptibility per mole of dinuclear complex is given as

$$\chi_m = (Ng^2\beta^2/3kT)[1 + \tfrac{1}{3}\exp(-2J/kT)]^{-1} \qquad (6)$$

N, g, β, and k have the usual meaning. The fitted lines are in excellent agreement with the experimental data. The corresponding fit parameters are listed in Table IV. For the red complex **2** a paramagnetic impurity of 16.7% has been taken into account, assuming $S = {}^1/_2$ and half the molecular weight of **2**. This agrees with the hfs in the $g = 2$ region of the solid-solution ESR spectrum of **2** in Figure 3, which originates from a doublet species. This impurity is responsible for the steep decrease of the susceptibility upon rising temperature above 4.2 K (Figure 5, line a). Subtraction of the impurity results in line b drawn below the experimental data in Figure 5A. The fits of the magnetic susceptibility in Figure 5 reveal antiferromagnetical exchange interactions, which in **2** are 1 order of magnitude stronger than in **5** (Table IV).

Discussion

All the reactions as reported above failed to synthesize the mononuclear complex CpVCot (**1**). It appears that this complex is not sufficiently stable to be isolated under normal conditions. In fact, the formation of the thermolabile exo-exo product **3** in (3), which in contrast to isomer **5** undergoes isomerization to **2** in (4), indicates the preformation of the desired mononuclear species **1** in the first step. Successively, an exo-exo ligand dimerization occurs which is normally found for 19 ve complexes (Scheme I).[27]

Several MO calculations have predicted that the free ligand e_2 orbitals of C_nH_n cyclopolyenes are progressively stabilized with increase in ring size.[28] Finally, this e_2 level is placed below the metal 3d levels in the case of Cot. Accordingly, as calculated for CpTiCot, the antibonding e_2* level lies closely above the singly occupied MO (SOMO).[28c] Considering the results of Fischer's MO calculations,[28a] the Cot-metal interaction in a CpVCot must be weaker than that in CpTiCot because of the more unfavorable relation of the ring size and the metal radius in the case of vanadium. A weaker interaction causes a smaller splitting of the bonding and antibonding combinations between the e_2 Cot and 3d metal orbitals in the V case. All things considered these effects may result in almost degenerate e_2, a_{1g}, and e_2* orbitals (Figure 6). Hence, the exo-exo ligand dimerization may be induced by a partial delocalization of one electron into the e_2* level if this level has substantial π-ligand character. However, this would certainly be in a contradiction to the INDO SCF calculation for CpTiCot which shows the e_2* orbital being of predominant metal character.[28c] A way out of this discrepancy could be an equilibrium between the 18 valence electron (ve) complex CpV(η^8-Cot) (**1**) and the triplet complex CpV(η^7-C_8H_8) with 17 ve on the metal center and one unpaired electron on the non-metal linked carbon atom (Scheme II).[29]

Scheme II

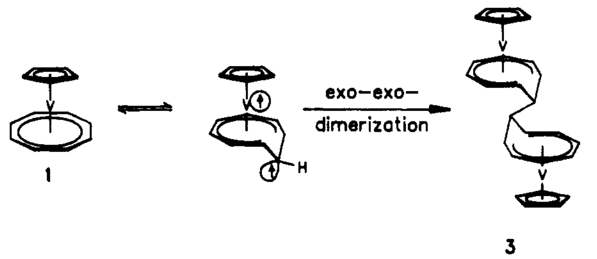

Scheme III

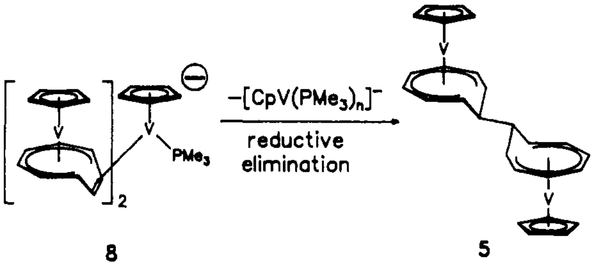

The thermal rearrangement of the green complex **3** to the red isomer **2** can be explained by means of a (metal assisted) 1,2-hydrogen shift as has been shown for CpV(η^7-C_8H_9) (**4**).[15]

The formation of the endo-endo isomer **5** is unique and needs special steric requirements to permit an endo-endo ligand dimerization. This may be achieved, if two [CpV(η^6-Cot)]$^-$ units are synfacially precoordinated to a third [CpV]$^+$-fragment (Scheme III, **8**). Subsequently this CpV fragment will be eliminated under reductive conditions in the presence of an excess of PR_3.[30,31] Work is in progress to confirm this suggestion.

The shallow boat conformation of the C_8 frame of the η^7-cyclooctatrienyl ligands in **2** as well as in **5**, which is also found in Cp*ZrC_8H_9[32] and in a dinuclear Ru complex,[33] structurally resembles the homotropylium cations.[34] The molecular structure

---

(26) (a) Van Vleck, J. H. *Electric and Magnetic Susceptibilities*; University Press: Oxford, England, 1932; p 182 ff. (b) Budreux, E. A.; Mulay, L. N. *Theory and Applications of Molecular Paramagnetism*; Wiley-Interscience: New York, 1976; p 352 ff. (c) Carlin, R. *Magnetochemistry*; Springer-Verlag: Berlin, 1986. (d) Bleany, B.; Bowers, K. *Proc. R. Soc. London, A* **1952**, *214*, 451.

(27) (a) Nesmeyanov, A. N.; Vol'kenau, N. A.; Shilovtseva, L. S.; Petrakova, V. A. *J. Organomet. Chem.* **1973**, *61*, 329. Andrianov, K. J.; Petrakova, V. A.; Struchkov, V. A.; Vol'kenau, N. A. *Koord. Khim.* **1986**, *12*, 978. Moinet, C.; Roman, E.; Astruc, D. *J. Organomet. Chem.* **1977**, *128*, C45. (b) Miller, P. M.; Widdowson, D. A. *J. Organomet. Chem.* **1986**, *303*, 411. (c) Adams, H.; Bailey, N. A.; Willet, D. G.; Winter, M. J. *J. Organomet. Chem.* **1987**, *333*, 61. (d) Zou, C.; Ahmed, K. J.; Wrighton, M. S. *J. Am. Chem. Soc.* **1989**, *111*, 1133. (e) Gaudet, M. V.; Hanson, A. W.; White, P. S.; Zaworotko, M. J. *Organometallics* **1989**, *8*, 286.

(28) (a) Fischer, R. D. *Theoret. Chim. Acta* **1963**, *1*, 418. (b) Cotton, F. A. *Chemical Application of Group Theory*; Wiley: New York, 1963. (c) Clack, D. W.; Warren, K. D. *Theor. Chim. Acta* **1977**, *46*, 313. Clack, D. W.; Warren, K. D. *Struct. Bonding* **1980**, *39*, 1.

(29) Astruc, D. *Chem. Rev.* **1988**, *88*, 1189.

(30) A synfacial linkage means the coordination of CpV fragments on the same side of the Cot ligand. A prospective synfacial coordination of two CpV units at one Cot ligand has just recently been shown by the formation of $(CpV)_2(\mu$-Cot),[4] which is produced in surprisingly negligible yield within reaction 5.

(31) Studies of Teuben et al. on the reactivity of $CpV^{II}PR_3$ compounds have shown the formation of stable vanadium alkene complexes. Within these studies hints were found for coupling products of olefins under reductive conditions (Hessen, B. Thesis, University of Groningen, Groningen, The Netherlands, 1989).

(32) Sinnema, P.-J.; Teuben, J. H. Personal communication.

(33) Goddard, R.; Woodward, P. *J. Chem. Soc., Dalton Trans.* **1980**, 559.

(34) Childs, R. F.; Faggiani, R.; Lock, C. J. L.; Mahendran, M. J. *J. Am. Chem. Soc.* **1986**, *108*, 3613. Childs, R. F. *Acc. Chem. Res.* **1984**, *17*, 347.

of 1-ethoxyhomotropylium 9^+ shows the same small bond angle of 101° at C8 and a drapery of the C_8 frame similar to that of the cyclooctatrienyl ligands in **2** and **5**, although the latter are more flattened due to the coordination of the C_8 ligand to the metal center. However, unlike 9^+ the homotropylium ligands in **2** and **5** do not show any systematical bond alteration and the mean bond length is enhanced from 1.385 to 1.405 Å, as expected for π-ligands upon coordination to metals.

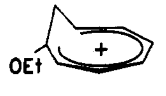

9^+

The almost identical UV/vis spectra of the mono- and dinuclear compounds **4** and **5** as well as the concurrence of the ESR data of **3**–**5** confirm a very close electronic relationship between these compounds. As pointed out earlier, the SOMO in **4** must be a singly occupied nondegenerate a_1 orbital with a preponderant V(d_{z^2}) character.[15] Hence, the same nature must be assumed for the SOMO in the CpV(η^7-C_8H_8) subunits of **3** and **5**. The fundamental difference between the mono- and dinuclear species is the triplet state of the latter removing the degeneracy of the ground state without an applied magnetic field. This zero-field splitting is among other things defined by the dipolar interaction D, which is determined by the isotropic exchange and the spin–orbit and the dipole–dipole interactions.[35] Since the exchange interaction parameter J of **5** is very small as well as the g anisotropy, which can be deduced from a comparison of the X- and Q-band spectra of **5**,[36] it is justified to take the dipole–dipole interaction into account only for the dipolar interaction D. From the predominant localization of the unpaired electrons in metal d_{z^2} orbitals of **3** and **5** they may be regarded as localized point dipoles. With this approximation D depends on the distance R between the paramagnetic centers and the angle θ between the magnetic field vector and the R vector in a randomly oriented matrix (eq 7).[37a]

$$D = [0.325 g_{\parallel}{}^2 R^{-3} |1 - 3\cos^2\theta|] \qquad (7)$$

R in Å; D in cm^{-1}

If we take $\theta = 0°$ because of the centrosymmetry of the dinuclear complexes, it is possible to determine R directly from D (eq 8).[37b,c]

$$R = [0.65 g_{\parallel}{}^2 D^{-1}]^{1/3} \qquad (8)$$

This approximation has been shown to be powerful in determining the intermetal distances of comparable dinuclear sandwich complexes in the triplet state.[25b,38] Taking the D values estimated directly from ESR spectra (see Table IV), the calculated distances R_{calcd} are distinctly larger (R_{calcd} (**5**) = 690 Å, R_{calcd} (**3**) = 660 Å) than those obtained from the X-ray data for **5** and estimated for **3** from a model based on the structural data of **5**, taking into account the exo–exo linkage and a trans conformation. This result may partially be due to the uncertainty of the zero-field-splitting parameter D obtained from the spectra and (or) to a conformational change of the compounds on going from the crystalline to the solid solution phase. In a trans conformation where a maximum metal–metal distance is already found, an additional elongation of the intermetal distance can only occur by means of a flattening of the angle between planes 1 and 2 of the homotropylium ligand, leading to smaller D values.

Scheme IV

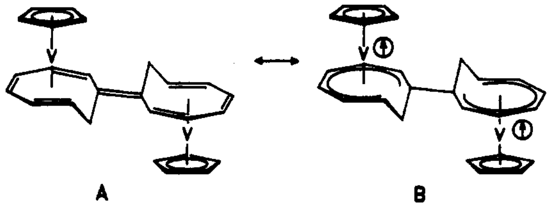

2

The almost identical structures of the mononuclear building blocks in the red and green isomers **2** and **5** imply a close relation of the nature of the SOMO in their CpV(η^7-C_8H_8) subunits. This is corroborated by the triplet state of these compounds and the comparable ^{51}V-hf coupling constants in the solid solution ESR spectra. However, a well-resolved fluid-solution ESR spectrum as recorded for **3** and **5** failed for **2**, although the dipole–dipole interaction must be expected to be small with respect to the large intermetal distance of 5.761 Å: for example, a well-resolved 15-line pattern is observed for the electronically related compound [μ-($\eta^{6:6}$-biphenyl)]bis[(η^6-benzene)vanadium] (**7**) in fluid solution (see Table IV), for which the V–V distance is even shorter (about 5.51 Å).[25b] If one determines the zero-field-splitting parameter D from the spectrum in Figure 3C with the same procedure as for **3** and **5**,[25a] D_{exptl} comes to 58 × 10^{-3} cm^{-1}, which is distinctly larger than calculated from eq 8 with R = 5.761 Å respecting dipole–dipole interaction only (D_{calcd} = 13.6 × 10^{-3} cm^{-1}). Even when the pseudodipolar coupling D_{pseudo} originated by the stronger exchange interaction J and the spin–orbit coupling[39] are considered, a dipolar coupling is revealed of about 24 × 10^{-3} cm^{-1} only, still less than half of the experimental value. The main distance between the unpaired electrons seems to be substantially smaller than indicated by the intermetal distance which is unusual for dinuclear sandwich complexes containing semioccupied orbitals of essentially metal d_{z^2} type.[25b,38] Such a decrease of the distance between the two unpaired electrons may be caused by a direct delocalization of spin density from the metal d_{z^2} orbital into the π-orbitals[40] of the C_8H_8 ligands augmented by the linkage of two sp^2 carbon atoms of the two C_8H_8 π-parts, which are also attached to the metal centers (structure I).

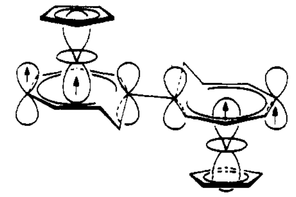

I

A more extensive delocalization also substantially contributes to the exchange interaction J. The bonding situation in **2** may therefore be described by two extremes as follows: (i) a diamagnetic, "low-temperature" valence structure with two V(d^4) centers linked via a heptaene ligand (Scheme IV, structure A), (ii) a paramagnetic, "high-temperature" structure consisting of a triplet state with two V(d^5) centers and a sp^2–sp^2 carbon–carbon single bond linking the two homotropylium ligands (Scheme IV, structure B).

Unlike the red compound **2**, the exchange interaction of the paramagnetic centers in **5** must occur via three carbon–carbon σ-bonds containing two sp^3 carbon atoms. Since spin density along carbon–carbon σ-bonds decreases dramatically,[41] a weak exchange interaction is expected. This is established by the small J value of -5 cm^{-1}. A comparable attenuation of the exchange interaction

---

(35) Kokoszka, G. F.; Duerst, R. W. *Coord. Chem. Rev.* **1970**, *5*, 209.

(36) Solid solution X- and Q-band ESR spectra of **5** are included in the supplementary material.

(37) (a) Chasteen, N. D.; Belford, R. L.; So, H.; Tapscott, R. E. *J. Am. Chem. Soc.* **1969**, *91*, 4675. (b) Chasteen, N. D.; Belford, R. L. *Inorg. Chem.* **1970**, *9*, 169. (c) Francesconi, L. C.; Corbin, D. R.; Clauss, A. W.; Hendrickson, D. N.; Stucky, G. D. *Inorg. Chem.* **1981**, *20*, 2059.

(38) Elschenbroich, Ch.; Heck, J. *J. Am. Chem. Soc.* **1979**, *101*, 6773. Heck, J. Dissertation, Philipps-Universität Marburg, Marburg, FRG, 1981.

(39) From an approximative axial complex D_{pseudo} can be estimated from the relation $D_{pseudo} \cong -J\{[(g_{\parallel} - 2)^2/4] - (g_{\perp} - 2)^2\}/8$ (see ref 37a). For $g_{\parallel}$ and $g\perp$, data of **4** were chosen.

(40) Clack, D. W.; Smith, W. *Inorg. Chim. Acta* **1976**, *20*, 93.

(41) (a) Wertz, J. E.; Bolton, J. R. *Electron Spin Resonance, Theory and Application*; McGraw-Hill: New York, 1972; p 87 ff. (b) Keller, H. J.; Schwarzhans, K. E. *Angew. Chem.* **1970**, *82*, 227.

is predicted by McConnell for the addition of a single carbon–carbon σ-bond between two paramagnetic centers,[42] which was experimentally verified for some diradicals.[37c,43] But the J value for **5** still complies with the condition of $|J| \gg |a_{iso}(^{51}V)|$, required for equal coupling of the two unpaired electrons with both V centers.[43]

The relatively large exchange integral in **2** compared with exchange interactions in fulvalene[44] and biphenyl-bridged dinuclear complexes, wherein the metal centers possess less than 18 ve,[25b,38,45] causes the assumption that generally stronger exchange interactions occur in complexes containing ligand systems which can be formally described as one polyene ligand linking two metal centers (structure II).

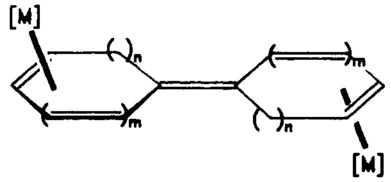

n = 0, 1...
m = 0, 1, 2...

II

Acknowledgment. We are greatly indebted to BASF for a donation of Cot and to the Fonds der Chemischen Industrie, Germany, for financial support.

Supplementary Material Available: A figure showing solid-solution X-band ESR spectra of **4** and **5** as well as a solid-solution Q-band spectrum of **5** (Figure 3D–F) and tables giving V–C and C–C bond lengths and angles of the CpV fragments and C–H bond lengths of **2** and **5** (Table 6), final fractional atomic coordinates and coefficients of isotropic thermal displacement factors of the hydrogen atoms (Table 7), anisotropic thermal displacement factors (Tables 8 and 9), and weighted least-squares planes through the cyclooctatrienyl ligands and equations of the planes (7 pages); tables of observed and calculated structure factors (27 pages). Ordering information is given on any current masthead page.

---

(42) McConnell, H. M. *J. Chem. Phys.* **1960**, *33*, 115.

(43) Briere, R.; Dupeyre, M. R.; Lemaire, H.; Morat, C.; Rassat, A.; Rey, P. *Bull. Soc. Chim. Fr.* **1965**, 3290. Dupeyre, M. R.; Lemaire, H.; Rassat, A. *J. Am. Chem. Soc.* **1965**, *87*, 3771. Glarum, S. H.; Marshall, J. H. *J. Chem. Phys.* **1967**, *47*, 1374.

(44) Schwarzhans, K. E.; Schottenberger, H. *Z. Naturforsch., B* **1983**, *38*, 1493 and literature cited therein. Sharp, P. R.; Raymond, K. N.; Smart, J. C.; McKinney, R. J. *J. Am. Chem. Soc.* **1981**, *103*, 753 and literature cited therein.

(45) For biphenyl-bridged dinuclear η^6-arene complexes consisting of 17 valence electrons on each metal center (see refs 25b, 38) the exchange parameter J is estimated from the temperature-dependent intensity of the half-field signal $\Delta m_s = 2$: $0 > J > -10$ cm^{-1} (Elschenbroich, Ch.; Heck, J. Unpublished results). For **2** a corresponding estimation of J leads to $J = -80 \pm 5$ cm^{-1}, which is in good agreement with the J value obtained from the susceptibility measurements.

Contribution from the Department of Chemistry,
Iowa State University, Ames, Iowa 50011

Two Novel Phases Containing Centered, Isolated Zirconium Clusters, $Rb_4Zr_6Cl_{18}C$ and $Li_6Zr_6Cl_{18}H$

Jie Zhang, Robin P. Ziebarth, and John D. Corbett*

Received August 6, 1991

The title compounds are synthesized by reaction of Zr, $ZrCl_4$ with RbCl plus graphite, or LiCl plus $ZrH_{1.7}$ at ~850 or 700 °C, respectively. Stability of the rubidium phase is marginal, and the synthesis requires excess zirconium. The structures of the two have been established by single-crystal X-ray diffraction: $Rb_4Zr_6Cl_{18}C$, $K_4Nb_6Cl_{18}$ type, $C2/m$, $Z = 2$, $a = 10.460$ (4) Å, $b = 17.239$ (4) Å, $c = 9.721$ (4) Å, $\beta = 115.05$ (3)°, $R(F)/R_w = 2.4/3.3\%$; $Li_6Zr_6Cl_{18}H$, $R\bar{3}$, $Z = 3$, $a = 15.969$ (1) Å, $c = 8.883$ (1) Å, $R(F)/R_w = 2.2, 2.5\%$. Individual close-packed layers of isolated $\{Zr_6(C)Cl^i_{12}Cl^a_6\}^{4-}$ clusters are present in the rubidium salt. However, the requirement of four cation sites results in offset, not close, packing of the layers, and the cations between these are bound more tightly to one layer than the other. The exo Zr–Cl^a bonds (2.59 Å) are the shortest known because of weaker $Cl^a \cdots Rb$ interactions. The rhombohedral $Li_6Zr_6Cl_{18}H$ contains cubic-close-packed $\{[Zr_6(H)Cl^i_{12}]Cl^a_6)^{6-}$ clusters with lithium in pseudooctahedral cavities between and within the layers. The Zr–cluster center distance, 2.257 Å, is at least 0.16 Å too large for good bonding of the hydride, and the solid-state ^1H NMR shift (~400 ppm vs $Fe^{3+}(aq)$ at room temperature) is similar to that in $Zr_6Cl_{12}H$ where a high hydrogen mobility is present. The sharp 11.8 ppm absorption in the ^7Li NMR spectrum (relative to LiCl) is consistent with the site symmetry deduced by X-ray diffraction and the nature of the nearest-neighbor chlorine atoms.

Introduction

The large collection of centered zirconium chloride cluster compounds $A_xZr_6(Z)Cl_{12}Cl_n$ owe their diversity to several factors. A considerable electronic variability is allowed by choices of both the number of valence electrons on the centering interstitial Z and the number (and charge) of the countercations within the cluster structure. A third variable provides the great structural variety exhibited by these compounds (as well as an electronic parameter), namely, the $0 \leq n \leq 6$ additional chlorine atoms that may be utilized in the essential Zr–Cl^a bonding exo to all six metal vertices of each $Zr_6(Z)Cl^i_{12}$ cluster unit. The sharing of chlorine atoms in this role between clusters necessarily joins these into network structures for all but for the limiting $n = 6$, where discrete $Zr_6(Z)Cl^i_{12}Cl^a_6$ ($=Zr_6Cl_{18}Z$) units pertain (i = inner, edge bridging; a = exo, terminal chlorine). The variables x, Z, and n thus afford numerous ways in which one can achieve, or come close to, the most favorable counts of cluster-based electrons, 14 with main-group (s, p) and 18 with transition-metal (d) interstitials in zirconium chloride clusters.[1-4]

The present article describes two of a small number of $A_xZr_6Cl_{18}Z$ phases known. Previous examples have been only $Rb_5Zr_6Cl_{18}B$[2] and an uncommon alkaline-earth-metal member, $Ba_3Zr_6Cl_{18}Be$,[5] although the $Zr_6Cl_{18}Z$ units in the latter are not quite as independent because of the higher charged cations. In fact, the latter compound is a proper member of a series $M_2M'Cl_6 \cdot Zr_6Cl_{12}Z$[6] ($=M_2M'Zr_6Cl_{18}Z$) in which each $Zr_6Cl_{12}Z$ cluster is bridged to others via six $M'Cl_6$ octahedra bonded at the exo positions. The original examples $M_2ZrCl_6 \cdot Zr_6Cl_{12}H$ with M = Na–Cs[7] thus contain $Zr_6Cl_{12}H$ clusters interconnected by

---

(1) Ziebarth, R. P.; Corbett, J. D. *Acc. Chem. Res.* **1989**, *22*, 256.

(2) Ziebarth, R. P.; Corbett, J. D. *J. Am. Chem. Soc.* **1989**, *111*, 3272.

(3) Rogel, F.; Zhang, J.; Payne, M. W.; Corbett, J. D. *Adv. Chem. Ser.* **1990**, *No. 226*, 369.

(4) Zhang, J.; Corbett, J. D. *Inorg. Chem.* **1991**, *30*, 437.

(5) Zhang, J.; Corbett, J. D. *Z. Anorg. Allg. Chem.* **1991**, *599/600*, 381.

(6) Zhang, J.; Corbett, J. D. To be submitted for publication.

0020-1669/92/1331-0614$03.00/0